

Preparation of $Ba_{1-x}Sr_xTiO_3$ thin films by metal-organic chemical vapor deposition and electrical properties

Jong-Guk Yoon, Soon-Gil Yoon, Won-Jae Lee, Ho-Gi Kim

Department of Materials Engineering, College of Engineering, Chungnam National University, Daeduk Science Town, 305-764, Taejeon, Korea.

Department of Ceramic Science & Engineering, Korea Advanced Institute of Science and Technology, Taejeon, Korea

(Received December 20, 1995)

ABSTRACT -- $(Ba_{1-x}Sr_x)TiO_3$ (BST) thin films have been grown on Pt-coated MgO by metal-organic chemical vapor deposition. X-ray diffraction results showed that BST films were grown on a Pt/MgO substrate with (100) preferred orientation perpendicular to the surface. The linear relationship of P-E curve obtained from hysteresis loop measurement indicated that the BST films had a Curie transitions below room temperature. Films deposited at 900°C exhibited a smooth and dense microstructure, a dielectric constant of 202, and a dissipation factor of 0.02 at 100 kHz. The leakage current density of the BST films is about 2×10^{-10} A/cm² at an applied electric field of 0.2 MV/cm. The electrical behavior on the current-voltage characteristics is well explained by the bulk-limited Pool-Frenkel emission.

I. INTRODUCTION

In recent years, ferroelectric thin films have been highly attractive with respect to application to dynamic random access memories (DRAM)¹⁾. $Ba_{1-x}Sr_xTiO_3$ (BST) which is a solid solution of $BaTiO_3$ and $SrTiO_3$ has a dielectric constants as high as 10,000 in bulk form²⁾. The Curie temperature of $BaTiO_3$ is shifted below room temperature with Sr concentration, thus making $(Ba_{1-x}Sr_x)TiO_3$ (BST) a room temperature paraelectric offering high dielectric constant, low leakage current, and large dielectric breakdown strength^{3, 4)}. Therefore, device using BST as a high permittivity dielectric can be operated at variable ambient temperature by precisely controlling the Sr concentration. Thin film devices have the advantage of low operating voltage which is always desirable for most potential applications. Therefore, large-scale fabrication technique for high quality thin films is requisite for the development of the device technologies using these types of materials.

To date, much of the thin film work on BST has involved physical vapor deposition techniques⁵⁻⁷⁾. However, several groups have reported the deposition of polycrystalline $BaTiO_3$ and $SrTiO_3$ by MOCVD^{8, 9)}.

The success of any MOCVD process depends critically on the volatility and stability of the precursor material. Until recently, complex strontium oxides have been prepared by $Sr(dpm)_2$ (dpm: dipivaloylmethanate; $C_{11}H_{19}O_2$) as Sr source³⁻⁵⁾. $Sr(dpm)_2$ used for complex strontium oxides have many disadvantages such as the decreased volatilities of the source by repeated thermal cycling near the melting temperature of $Sr(dpm)_2$.

Therefore $Sr(hfa)_2$ (tetraglyme) (hfa: hexafluoroacetylacetonate; $C_5HF_6O_2$) which exhibits significantly improved volatility and vapor pressure stability was used in this study. This study reports that MOCVD has been successfully employed to deposit BST thin films on Pt/MgO. The structure and electrical, dielectric properties of BST films were evaluated and discussed.

II. EXPERIMENTAL PROCEDURE

The success of any MOCVD process depends critically on the stability of the metal-organic precursor material. For this study, we have used $Ba(hfa)_2(tet)$ and $Sr(hfa)_2(tet)$ [(hfa = hexafluoroacetyl-acetate; $C_2HF_6O_2$); (tet = tetraglyme)] as precursors for the barium and strontium sources, respectively. Titanium tetraisopropoxide (TPT) was also chosen as the Ti source. MgO substrates were used to investigate the preferred orientation of films. Deposition was carried out at a system pressure of 4 Torr and a high substrate temperature of 800-900°C because SrF_2 second phase was formed below 800°C. The evaporation temperature of $Ba(hfa)_2(tet)$, $Sr(hfa)_2(tet)$, and TPT were maintained at 120°C, 120°C and 30°C, respectively. The sources were transported to the reaction zone by an argon carrier gas at flow rate of 80 sccm for $Ba(hfa)_2(tet)$, 80 sccm for $Sr(hfa)_2(tet)$, and 20 sccm for TPT. The film thickness was determined by using the cross-section scanning electron microscopy (SEM). X-ray diffraction (XRD) using $Cu K\alpha$ radiation was used to determine the crystal phase and preferred orientation of the films. The electrical properties of the BST films were performed by current-voltage (I-V), capacitance-voltage (C-V), dielectric constant and dissipation factor versus frequency. they were carried out in metal-insulator-metallic (MIM) configurations, where the top electrode of Pt with a diameter of 0.3 mm were prepared by dc sputtering.

III. RESULTS and DISCUSSION

Fig. 1 shows the XRD patterns of BST films deposited at different substrate temperatures. As shown in Fig. 1, single phase of BST film above 850°C was obtained. However, $BaTiO_3$ and TiO_2 second phases were formed at 800°C. Fig. 2 shows the relationship between the texture coefficient and the deposition temperatures. In order to investigate

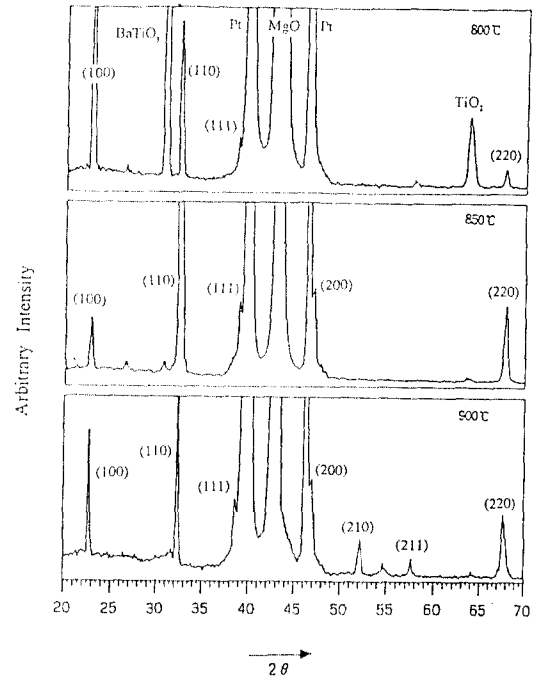


Fig. 1. XRD patterns of BST films deposited on Pt/MgO at different substrate temperatures.

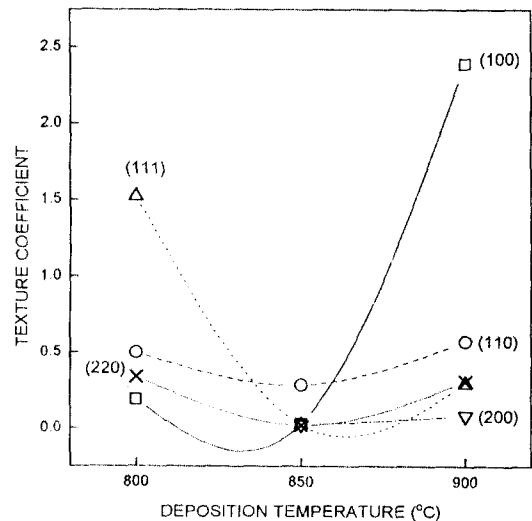


Fig. 2. Texture Coefficient of BST films with various deposition temperatures

the preferred orientation of the deposition layer, texture coefficient $TC(hkl)$ of each plane is obtained using the Hariss method^[10] as follows;

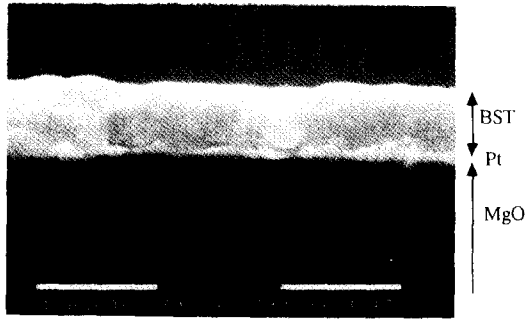


Fig. 3. Cross-Sectional Image of BST films deposited on Pt/MgO at 900°C.

$$TC(hkl) = \frac{I(hkl)}{I_o(hkl)} \left[\frac{1}{n} \sum_I \frac{I(hkl)}{I_o(hkl)} \right]^{-1} \quad (1)$$

Where $I_o(hkl)$ is the standard intensity of the (hkl) plane, $I(hkl)$ is the measured intensity of the (hkl) plane, and n is the number of reflections. Equation (1) shows that $TC(hkl)$ of each crystal plane is unity for a randomly distributed powder sample while $TC(hkl)$ of each crystal plane is larger than unity for the preferred growth.

Texture coefficient analysis reveals that the BST deposit has a (100) preferred orientation with increasing deposition temperatures. We believe that the increase of (100) preferred orientation is due to increasing surface diffusion as the deposition temperature increases. Fig. 3 shows the cross-sectional SEM image. The films have a dense and smooth structure. The fracture surface shows that the films consist of $(Ba, Sr)TiO_3$ and crystalline Pt layer. Fig. 4 shows the capacitance-voltage characteristics of BST film versus dc bias at a measuring frequency of 100 kHz. It may be seen that the capacitance was not affected significantly by the electric field within the region of applied voltage $\pm 3V$. This curve was measured with both increasing and decreasing bias voltage, and a hysteresis was not observed. This indicates that the dielectric films are not ferroelectric, and that they contain no mobile ions. The hysteresis loops for polycrystalline BST film were shown in Fig. 5

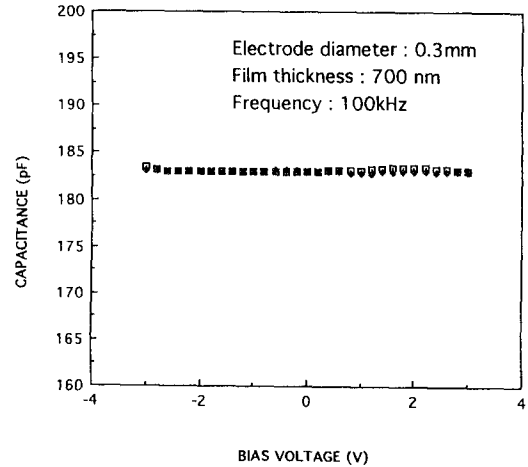


Fig. 4. Capacitance-Voltage Characteristics of BST/Pt/MgO film deposited at 900°C.

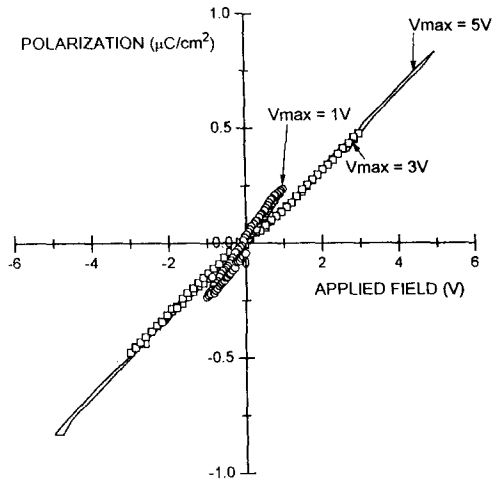


Fig. 5. Hysteresis Characteristics of BST film deposited on Pt/MgO at 900°C with different maximum voltage.

with increasing the maximum voltage. As shown in Fig. 5, The obtained hysteresis loops indicated that the BST films have a paraelectric properties at room temperature. Therefore, this result suggested that the Curie temperature of BST film exhibited below room temperature. From this result, we can calculate the charge storage density Q_c using the following equation because BST is a paraelectric material at room temperature:

$$Q_c = \epsilon_0 \cdot \epsilon_r \cdot E$$

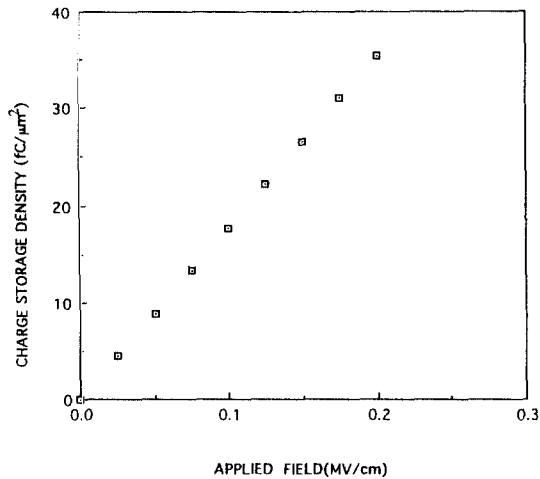


Fig. 6. Charge Storage Density of BST film as a function of applied field.

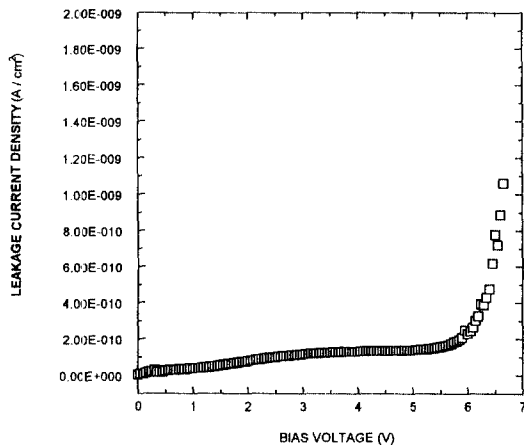


Fig. 7. Leakage Current Density of BST film deposited at 900°C as a function of applied voltage.

Where ϵ_0 and ϵ_r are the dielectric permittivity of vacuum and the dielectric constant of $(Ba, Sr)TiO_3$ film, respectively. E is the applied electric field. The relation between applied electric field and the calculated charge storage density was shown in Fig. 6. The charge storage density was calculated from capacitance-voltage measurements on MIM capacitors. The films have a Q_c of about 35 $fC/\mu m^2$ at an applied field of 0.2 MV/cm. Fig. 7 and 8 show the I-V characteristics of the BST film.

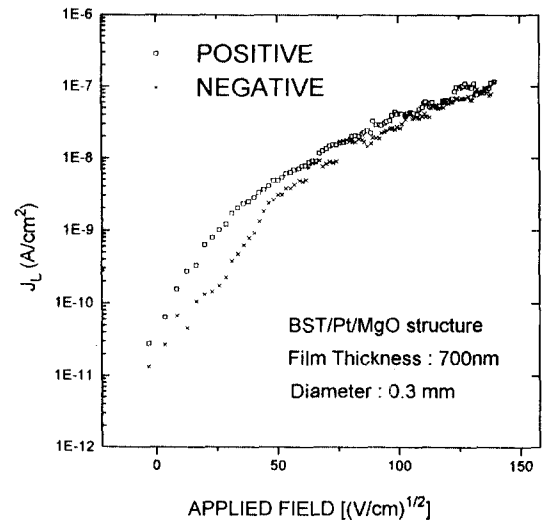


Fig. 8. $\log(J_L)$ vs $E^{1/2}$ plot of the films deposited at 900°C.

As shown in Fig. 7, at the low voltage region, the leakage current density is nearly linear to the applied voltage. However, at the high voltage region, the electrical behaviors become very nonlinear. The I-V characteristics at low-field region indicated that the ohmic characteristics of current flow is dominate in this regions. The nonlinear relationship in the high voltage region suggested the existence of other conduction mechanisms. To identify the mechanism, $\log(J_L)$ versus $E^{1/2}$ was plotted as shown in Fig. 8. At low electric field, magnitude of currents depended on the polarity of the applied voltage. However, at high electric field, currents from both directions approach each other and the plot of $\log(J_L)$ vs $E^{1/2}$ showed a linear relationship. It is known that the field-enhanced Schottky emission and the Poole-Frenkel emission result in a linear relationship between $\log(J_L)$ and $E^{1/2}$ ¹¹⁾. The Schottky emission results from field-induced lowering of the potential barrier at the metal-dielectric interface. The Poole-Frenkel emission is associated with field-enhanced thermal excitation of trapped electrons (ionization of trap) into the conduction band. Hence, the Schottky emission is electrode-controlled and the current can be de-

pendent on the polarity of the applied voltage at high voltage region, while the Poole-Frenkel emission is bulk-controlled and the current does not depend on the polarity at high applied voltage region. In this result, Virtually identical currents from both directions at a high voltage region suggest that the Poole-Frenkel emission is responsible for the current-voltage characteristics.

IV. CONCLUSIONS

The polycrystalline $Ba_{1-x}Sr_xTiO_3$ film has been successfully grown on Pt/MgO substrates by MOCVD technique. MOCVD derived BST films exhibited a Curie transitions below room temperature from the P-E hysteresis loop measurements. A leakage current density of 2×10^{-10} A/cm² and a charge storage density of 35 fC/ μm^2 at a field 0.2 MV/cm were obtained with films of 500 nm thickness. BST films showed two different transport mechanisms of Ohmic and bulk-limited Poole-Frenkel emission from the I-V characteristics.

REFERENCES

1. S. Yamamichi, T. Sakuma, K. Takemura, and Y. Miyasaka, *Jpn. J. Appl. Phys.* **30**, 2193 (1991).
2. E. N. Bunting, G. R. Shelton and A. S. Creamer, *J. Res. Nat. Bur. Std* **38**, 337 (1947).
3. L. A. Araujo, L. C. Mcmillan, B. M. Melnick, J. D. Cucharo, and J. F. Scott, *Ferroelectrics* **104**, 241 (1990).
4. R. Moazzami, C. Hu, and W. H. Shepherd, *IEEE Electron Device Lett.*, **EDL-11**, 454 (1990).
5. K. Fujimoto, Y. Kobayashi, and K. Kuboto, *Thin Solid Films*, **173**, L139 (1989).
6. Z. Surowiak, T. S. Nikitin, S. V. Biryukov, I. I. Golovko, V. M. Mukhortov, and V. P. Dudkevich, *Thin Solid Films*, **208**, 77 (1992).
7. S. Xamamichi, T. Sakuma, T. Hase, and Y. Miyasaka, *Mat. Res. Soc. Symp. Proc.*, **243**, 297 (1992).
8. B. S. Kwak, K. Zhang, E. P. Boyd, A. Erbil, and B. J. Wilkens, *J. Appl. Phys.*, **69**, 767 (1991).
9. W. A. Feil, B. W. Wessels, L. M. Tonge, and T. J. Marks, *J. Appl. Phys.*, **67**, 3858 (1990).
10. C. Barret and T. B. Massalski, "Structure of Metals" P 204, Pergamon Press, Ltd, Oxford (1980).
11. S. M. Sze, "Physics of semiconductor Devices", John Wiley & Sons, New York, (1981).